COMPUTERS AND BIOMEDICAL RESEARCH 16, 273–286 (1983)

A Robust-Digital QRS-Detection Algorithm for Arrhythmia Monitoring

ADRIAAN LIGTENBERG AND MURAT KUNT

Signal Processing Laboratory, Ecole Polytechnique Fédérale de Lausanne, 16 ch. de Bellerive, CH-1007 Lausanne, Switzerland

Received June 25, 1982

The success of automated patient monitoring is primarily dependent on the ability to detect normal as well as bizarre QRS-complexes. In this paper a new robust single lead QRS-detection algorithm is presented. The QRS detector can be separated into five different blocks, namely, a noise filter, a differentiator, an energy collector, a minimal distance classifier, and a minimax trimmer. Each block accounts for some characteristic features of QRS complexes (steepness, duration, etc.). The time delay introduced by this algorithm for making a decision is less then one second, allowing real-time applications. The performance of the QRS detector is analyzed and results are presented.

I. INTRODUCTION

One of the most essential steps for the successful analysis of electrocardiograms (ECG), employed by ECG specialists as well as in automated techniques, is the detection of the basic heart rhythm (*1*). This rhythm can be derived from the position on the time scale of successive QRS complexes. Once the position of the QRS complex is known, a more detailed examination of the signal can be carried out to study the complete cardiac period.

Noise sources such as baseline wandering, powerline interference, muscle tremor, and artifacts will affect the performance of the QRS detector at one hand and peaky tented *T* waves and small premature ventricular contractions (PVC) will cause ambiguity at the other.

A large number of QRS-complex detectors, as well as improvements of existing schemes, have appeared in literature. Several of these QRS-detection schemes minimize the influence of some noise sources as mentioned above. In general, QRS-detection schemes can be divided into three main categories: thresholding algorithms (*2–5*), matching algorithms (*6–7*), and syntactical algorithms (*8, 9*). The first ones have the advantage that they can be implemented easily due to their relative simple structure. However, the selection of the threshold values is quite arbitrary and patient dependent. If no special

0010-4809/83 $3.00

precautions are taken, the resulting performance will not give full satisfaction. The performance of matching algorithms depends on a priori knowledge of the templates and is therefore a trade-off between memory capacity and computation time on one side and reliability on the other. Although the syntactical algorithms are regarded as the most promising schemes, the reported results hitherto are not convincing. A reason for this is the simplification required to avoid the heavy computation load involved in complex schemes.

For on-line monitoring of cardiac patients there is still a need for a reliable and accurate automated QRS-complex detection algorithm. Fortunately, the evolution of VLSI technology (very large scale integration, e.g., microprocessors and memory chips) makes it possible to detect QRS complexes on-line exploiting advanced (complex) pattern recognition techniques.

In Section II we introduce the new QRS-detection algorithm. A performance measure is defined in Section III to evaluate the contributions of the different stages in the QRS detection, whereas in Section IV the results are presented. Finally, a concluding discussion is given in Section V.

II. The QRS-Complex Detection Method

The normal QRS complex is a pronounced feature within the ECG signal. It is characterized by steep slopes and has a duration varying from 0.07 to 0.10 sec in general. An analysis of the frequency content (*6*) shows that the major part of the energy is distributed between 10–30 Hz.

QRS detectors should take into account at least some of the above mentioned characteristics; besides this, it may not ignore different shaped QRS complexes found for some arrhythmia. Figure 1 shows the block diagram of the digital QRS detector. Different blocks can be distinguished.

(1) *Noise filter* (*10*). Its main purpose is to eliminate baseline drift and powerline interference, and to attenuate artifacts. The filter consists of two branches, each containing two moving average filters in cascade. This results in a simple bandpass filter structure and has the advantage that it can be implemented recursively. The output $y(k)$ of this filter is given by

$$y(k) = \frac{1}{K^2} \sum_{m=k-K+1}^{k} \sum_{n=m-K+1}^{m} x(n) - \frac{1}{L^2} \sum_{m=k-L+1}^{k} \sum_{n=m-L+1}^{m} x(n) \qquad [1]$$

where K and L are two constants and $x(n)$ the input signal. In our case, with a sampling rate of 250 Hz, $K = 5$ and $L = 200$. The frequency characteristic $H(f)$ is given by

$$H(f) = \frac{1}{K^2} \left(\frac{\sin \pi f K}{\sin \pi f} \right)^2 \exp[-2j\pi f(K-1)] - \frac{1}{L^2} \left(\frac{\sin \pi f L}{\sin \pi f} \right)^2 \exp[-2j\pi f(L-1)]. \qquad [2]$$

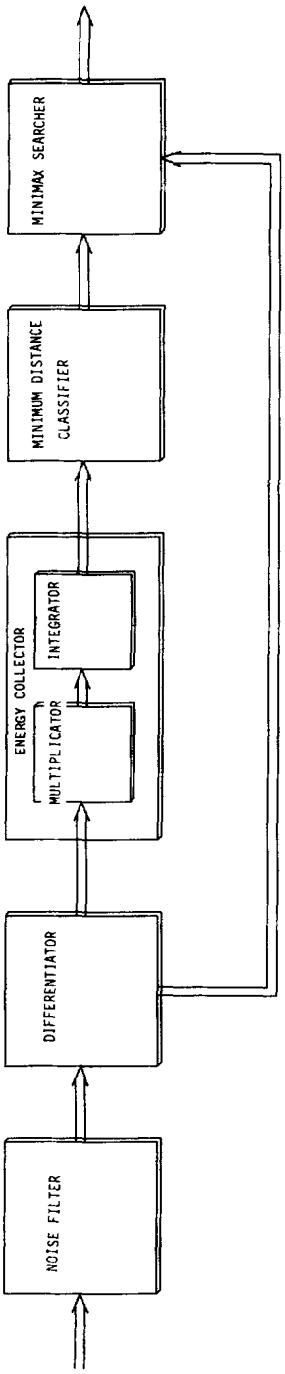

FIG. 1. Block diagram of the QRS-complex detector.

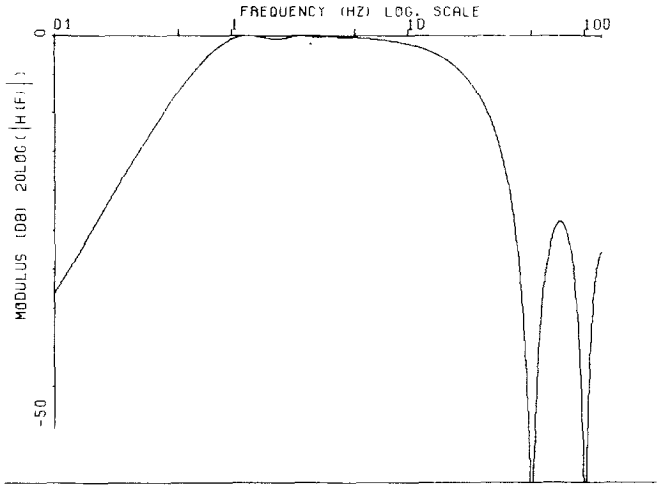

FIG. 2. Frequency characteristics of the noise filter.

Figure 2 shows the bandpass frequency characteristic. The elimination of the 50-Hz a–c component and its harmonics is clearly seen.

(2) *Differentiator.* To account for the steep slopes of the QRS complex as well as for accurately computing the position of the R peak, we make use of a differentiating algorithm. An ideal derivative will be characterized by a straight 45-degree line in the frequency domain. An ideal derivative is not convenient for our purpose, because the frequency content of the QRS complexes is limited; it will amplify the high frequency noise. Therefore a band limited differentiator is preferred. Equation [3] gives the weighted impulse response h_d coeffi-

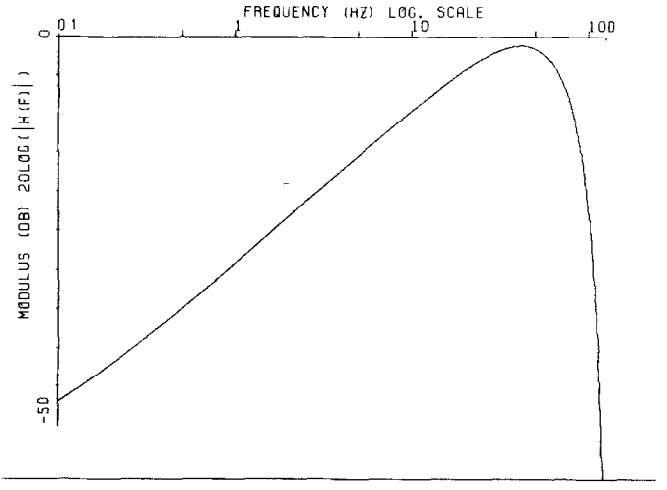

FIG. 3. Frequency characteristics of the differentiator.

cients and the frequency characteristic of a band limited derivator. Figure 3 shows its frequency characteristic. The straight 45-degree line for the lower frequencies as well as the rapid fall-off for the higher frequencies can be distinguished. From the samples surrounding the zero crossings of the derivate, the position of the maximum corresponding to the R top can accurately be interpolated

$$h_d = \tfrac{1}{8}(-1, -2, 0, 2, 1,)$$
$$H(f) = \tfrac{1}{8}\sin(4\pi f) + \tfrac{2}{8}\sin(2\pi f). \qquad [3]$$

(3) *An energy collector.* The energy collector is composed of a squarer followed by a moving average integrator. The nonlinear squarer can be considered as a convolution in the frequency domain. This means that strong frequency components are favored. The integrator accounts for the duration of the QRS complex. The energy collector is governed by the equations

$$y_a(k) = \{x_a(k)\}^2 \qquad [4]$$

$$y_b(k) = \sum_{n=k-N+1}^{k} x_b(n) \qquad [5]$$

where N is the number of samples used for integration, $x(\ )$ is the input, and $y(\ )$ the output signal.

(4) *An adaptive minimum distance classifier.* The output of the energy collector will be used to identify the QRS complexes. Therefore, the "global" maxima of the energy values in a 15-point window are determined and a classification is carried out as described below. (The 15-point window is used to reduce the set of elements involved in the classification.) The "global" maxima are composed of the contributions of two classes: the QRS class (QRS) and the nonQRS class ($\overline{\text{QRS}}$). The distance of the maxima (y_b) to the mean values (μ) of the two class centers is computed and a minimal distance classifier is applied. After the classification the values of the mean cluster centers are adapted according to the equations

$$\mu_{\text{QRS}}(k) = 0.9\ \mu_{\text{QRS}}(k-1) + 0.1 y_b \qquad [6a]$$

$$\mu_{\overline{\text{QRS}}}(k) = 0.9\ \mu_{\overline{\text{QRS}}}(k-1) + 0.1 y_b \qquad [6b]$$

depending on whether the value y was classified as an element of the QRS class (Eq. [6a]) or the nonQRS class (Eq. [6b]). The adaptation is needed to be able to follow changes in the morphology of the QRS complexes. As initial conditions, the minimal and maximal values of the first two seconds of the energy are used for the two cluster centers.

(5) *A minimax searcher.* If a QRS complex is found by the classifier operating on the energy signal, the corresponding positions in the nearest zero crossings in the derivative are determinated and the interpolated value of the ECG signal

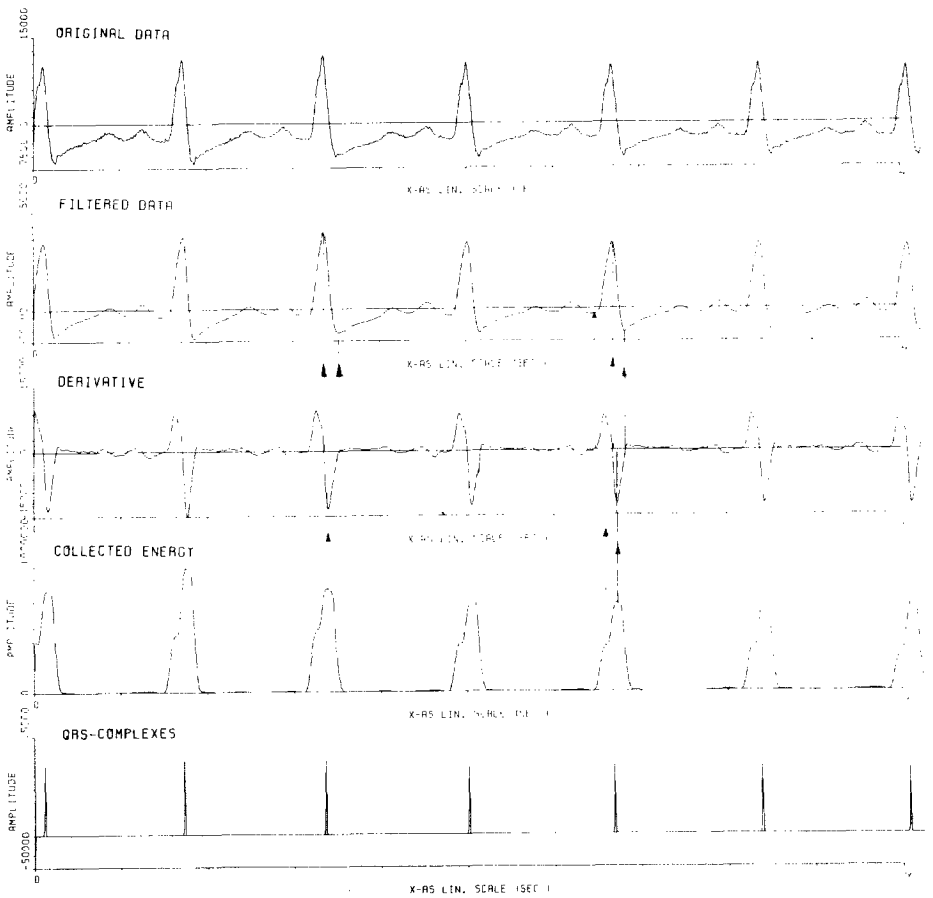

FIG. 4. Original ECG data as well as the output signals of various blocks. The arrows indicate the path followed by the minimax trimmer. Even a correct classification is found for nonglobal maxima, as shown by following the broken arrow.

will be identified as R top if it is a maximum and as S top if it is a minimum. Figure 4 depicts these successive steps.

An important characteristic of the algorithm is the time necessary after arrival of an input sample to decide if a QRS complex is present or not. The time elapsed before making a decision is less than one second. The contributions to this time delay of the various stages in the QRS-detector scheme are a delay of 200 samples caused by the noise filter, 2 samples needed by the differentiator, 7 samples introduced by the energy collector, 7 samples necessary for the classifier, and a variable number for the minimax searcher; however, this number will never exceed 10 samples. The major part of the time delay (200 samples) is introduced by the noise filter and is due to the fact that the lower frequency cutoff of the bandpass characteristic is chosen to be 1.25 Hz. The time delay

can be reduced because a higher value of the lower cutoff frequency will not effect the QRS-detection result. This can be seen from the frequency characteristic (Fig. 3) of the following block, the differentiator; it effectively attenuates frequency components onto about 10 Hz. The reason the lower cutoff frequency is established on 1.25 Hz is that it eliminates the baseline variations while conserving important characteristics of the ECG signal (*10*). This filtered signal can be used to study the ECG in more detail.

III. Performance Measures

To evaluate QRS-detection schemes, the a priori knowledge of the distributions of features which distinguish the QRS-complex and nonQRS-complex classes would be very useful. It permits definition of an optimal decision rule based on the minimization of the Bayes error. Unfortunately, this information is not available. A second method, statistical in nature, is usually applied. A large amount of ECG data is processed by the QRS detector and the results are compared with those of a careful examination by the cardiologist. The result has an important but restricted value because it indicates the type of classes of QRS complexes for which the method is applicable but does not give any indication about the QRS classes not involved in the measurement or the absolute separation strength of the algorithm. There is no trivial way to solve the problem of the unknown QRS classes. Modeling of QRS complexes can be helpful herein. The separation between the two classes can be measured by applying statistical methods.

An objective performance measure of the separation strength is the class distance β between the two classes, defined as

$$\beta = |\mu_1 - \mu_2| - \alpha\{\sigma_1 + \sigma_2\} \qquad [7]$$

where μ_1 and μ_2 are the mean values and σ_1 and σ_2 are the standard deviations of the QRS-class and nonQRS-class clusters, respectively. The parameter alpha permits us to weigh the influence of the dispersion of the distributions. A value of alpha equal to three is used in our experiment. This means that under the assumption that the distributions are normal, a $\beta = 0$ tolerates 0.13% false positives (FP) and 0.13% false negatives (FN).

FP = probability of QRS detection if no QRS complex is present

FN = probability of nondetection if QRS complex is present.

The maximal threshold value which gives no FP in terms of error probabilities will be determined. The FN can be easily removed in a later state of the processing.

IV. Experimental Results

Three segments of five-minute registrations of different natures obtained from three patients were analyzed. The ECG signals are sampled with 250 Hz

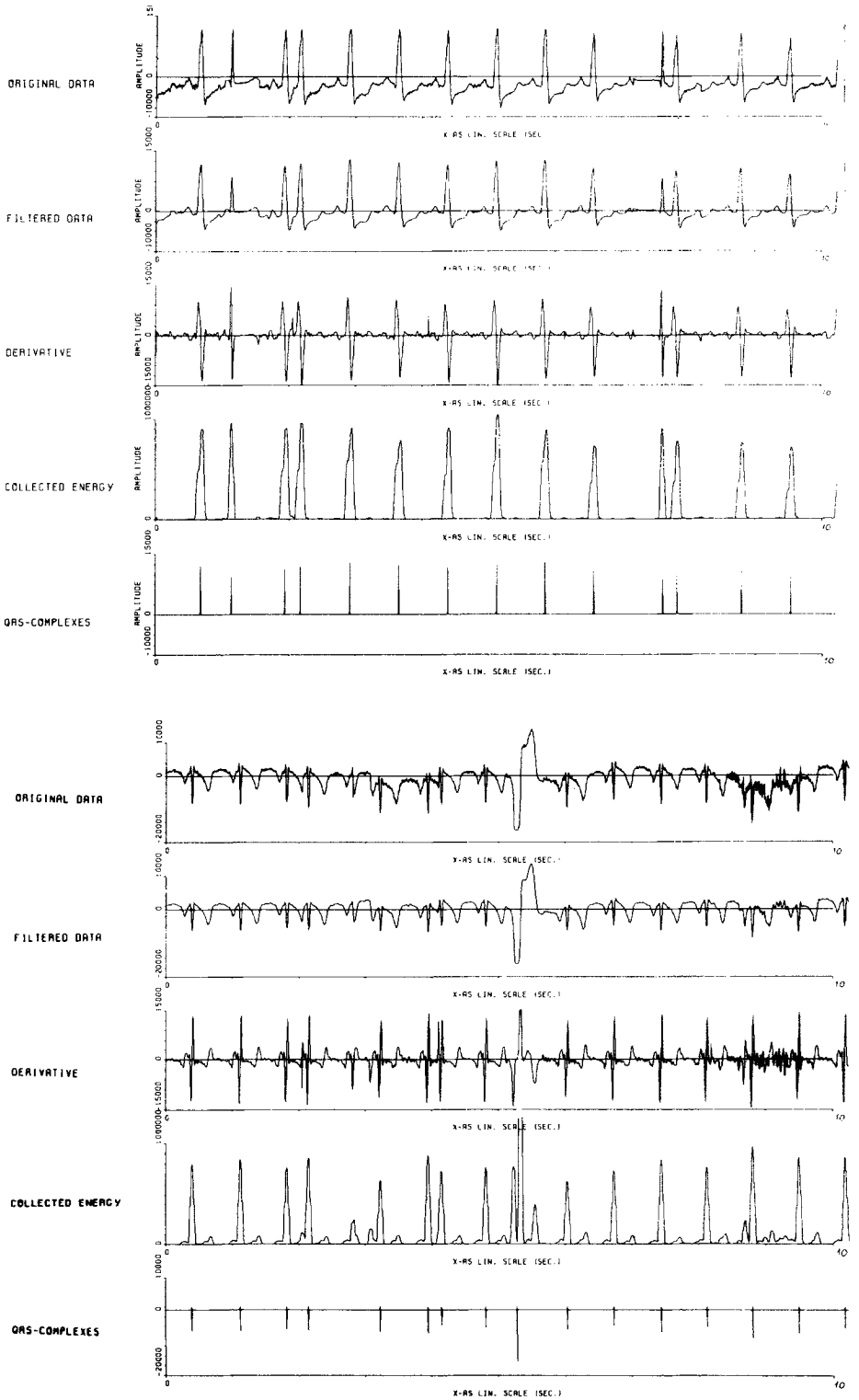

FIG. 5. Typical parts of two different registrations as well as the signals obtained after successive stages of the QRS-complex detector. The only FN can also be seen.

and quantized with 10 bits. Figure 5 shows some typical waveforms, together with the successive results obtained after the processing by the first three blocks of the QRS detector. The QRS detector produced one FN and one FP.

To evaluate the contributions of the first three blocks, the histograms of the minimal and maximal values of the various signals involved in the QRS detector are determined for the entire registration. To create the histogram of the output derivative, the absolute values of the differentiator are used. This is possible because the sign information of the derivative is not relevant. The values representing the QRS complexes for the different blocks are determined and the corresponding histogram is computed. For the derivative, each QRS complex is characterized by two values, the maximal value of the on and down slopes, respectively.

TABLE I

OVERVIEW OF THE PERFORMANCE OF THE FIRST THREE BLOCKS OF THE QRS-COMPLEX DETECTOR

	Number of QRS Complexes		Threshold		P(QRS)	P(QRS)[b]	Performance
	Real	Analysis set	Position (units)	FN/FP[a]	μ/σ^2	μ/σ^2	β[c]
Patient 1	355						
Original data		11513	338	1/0	395/64	238/117	100
Filtered data		4224	331	0/0	357/27	252/45	69
Derivative data		7729**	117	9/0	343/594	7/207	219
Collected energy		3338	351	4/0	457/758	2/347	316
Patient 2	390						
Original data		8414	352*	16/0*	383/385	223/523	32
Filtered data		3307	331*	1/0*	386/374	244/443	20,8
Derivative data		6302**	169	30/0	285/5533	21/730	−40
Collected energy		3454	305	56/0	403/2753	28/5367	−2
Patient 3	426						
Original data		9982	209*	1247/0	149/1556	257/1066	−108
Filtered data		3886	211*	461/0	185/925	261/962	−108
Derivative data		7268**	2	6416/0	312/1684	41/1677	24,8
Collected data		3616	200	29/0	366/3398	20/1406	58,6
Total (1, 2, 3)	1171						
Original data		29909	209*	3653/0	301/14101	240/728	−376
Filtered data		11417	211*	856/0	304/8681	253/512	−296
Derivative data		21299**	2	18769/0	312/3186	22/1060	23
Collected energy		10408	200	174/0	406/3763	17/2496	55

[a] FP: false positive; FN: false negative.

[b] P(QRS): distribution QRS class; P($\overline{\text{QRS}}$): distribution nonQRS class; μ: mean; σ^2: variance.

[c] β: $|\mu_1 - \mu_2| - 3|\sigma_1 + \sigma_2|$.

* Threshold placed on absolute value.

** One QRS complex is characterized by two values (up and down slope).

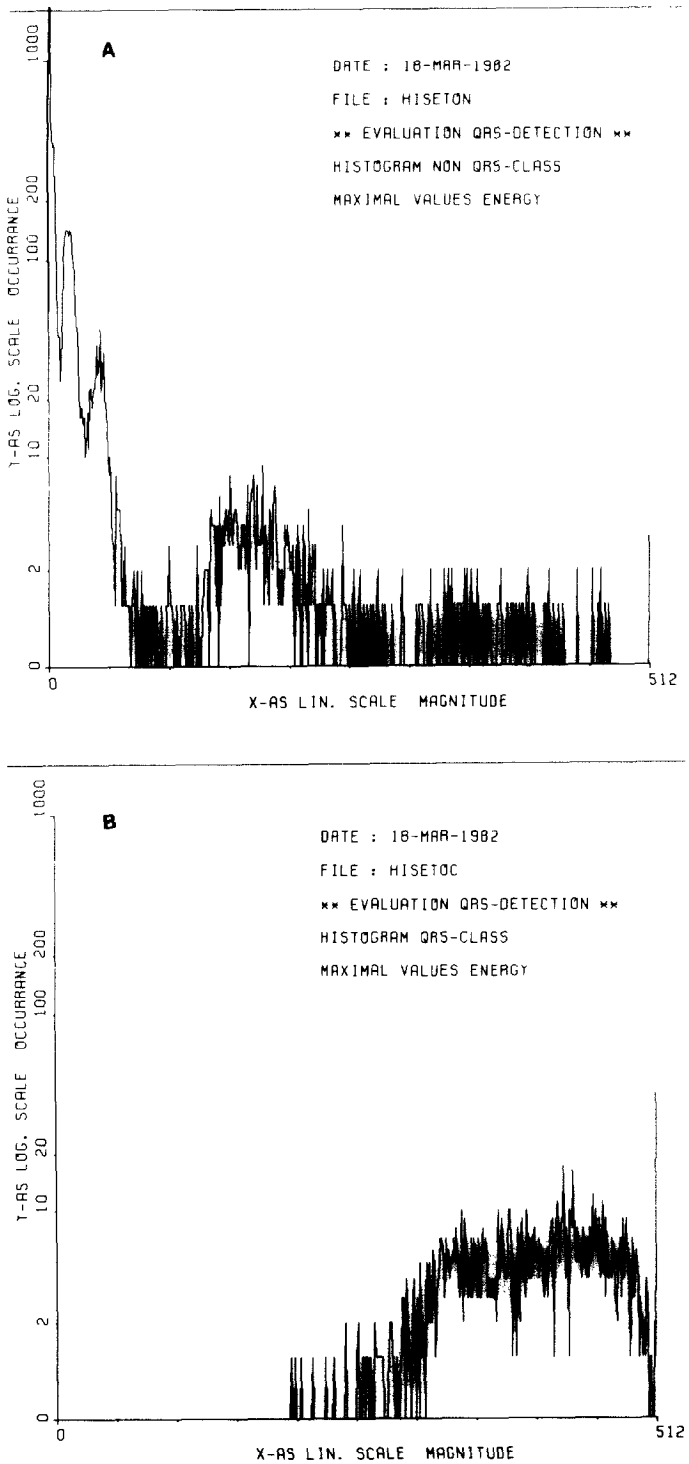

FIG. 6. The histogram of the maxima in the energy values cumulated for the three patients on the right together with the separate distributions of the QRS class and the nonQRS class, respectively, in the middle and on the left.

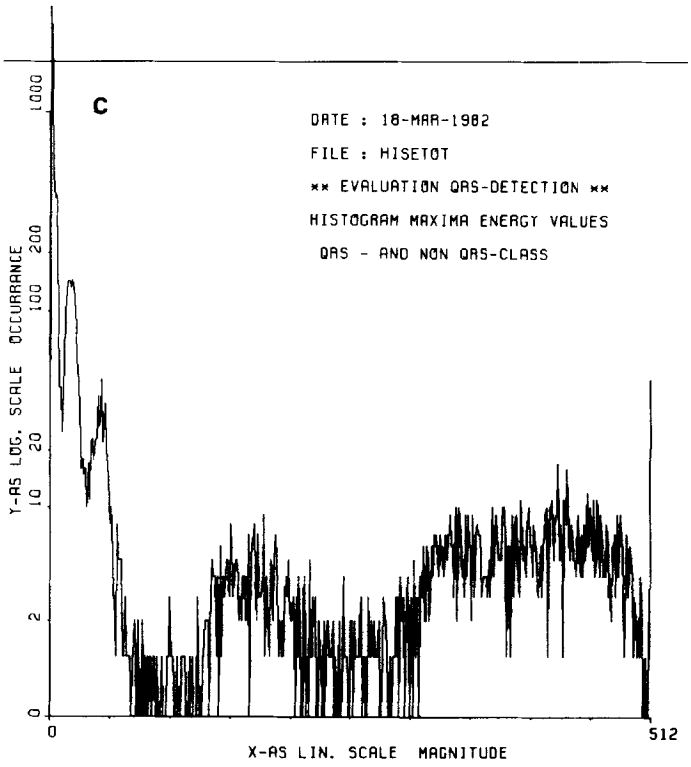

FIG. 6—*Continued.*

The histograms of the QRS class and nonQRS class of the cumulative maximal energy values for the three registrations are shown in Fig. 6. There is still an overlap between the QRS and nonQRS classes. However, the improvement in separability compared with the histograms obtained after noise filtering and differentiation is great, as can be seen from Fig 7. Figure 7 presents an overview of the distributions after successive operations of the QRS detector for the three patients. The class distance and the maximal position of the threshold which caused no FP are computed and the remaining FN are determined. The results are summarized in Table I.

An analysis of Table I and Fig. 7 shows the improvement obtained by combining the different blocks. The noise filter reduced the number of potential QRS complexes in the analysis set and the variance in the distributions. The price paid for this is the decrease of the distance between cluster centers which reduces the performance β. The fact that, with a simple, well-placed threshold, the performance in terms of FP/FN is quite reasonable for two patients is remarkable. Differentiation improves the distance between the mean cluster centers. Unfortunately, the variance increases too, especially for patient 2, showing intraventricular conduction disturbances, causing a widening of the

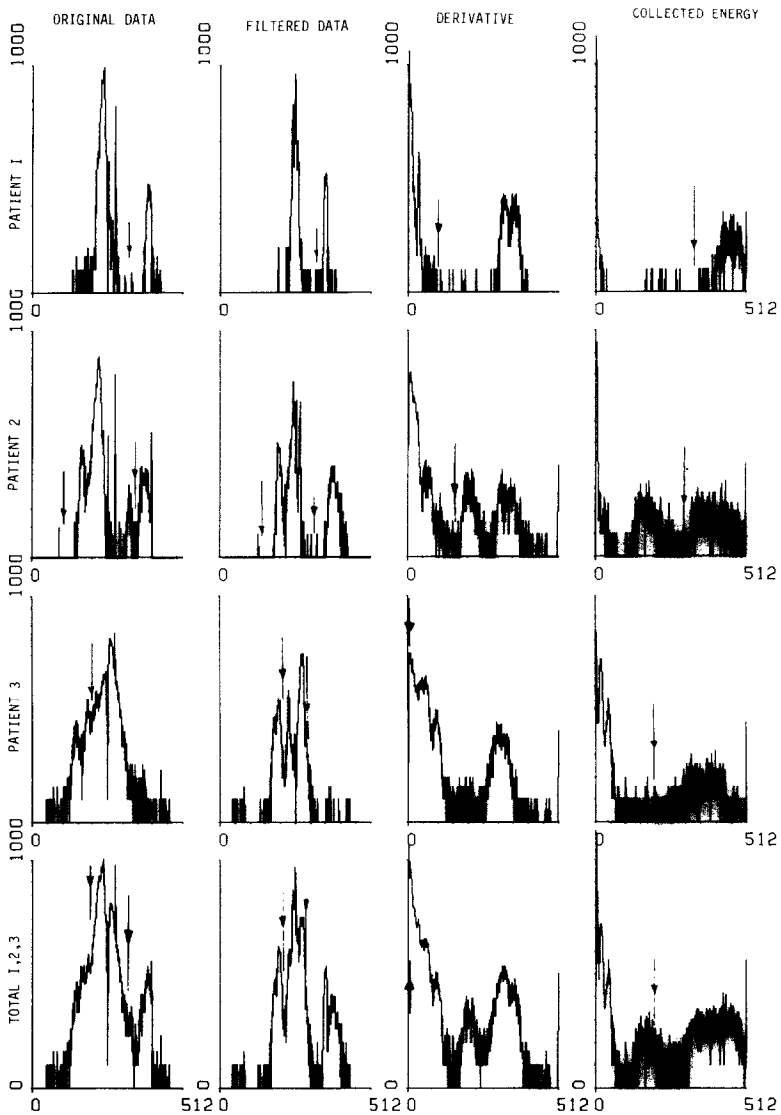

FIG. 7. An overview of the histograms after successive operations of the QRS detector for the three registrations. On the linear x scale is found the normalized magnitude, and on the logarithmic y scale the occurrence.

QRS complex, and resulting in different values for the up and down slopes. The collected energy has the best total performance. The distance between the cluster centers is enlarged. Although the number of FN is still high, it is not dependent on the morphology of the waveforms. For this reason an adaptive classifier is applied to the magnitude of the collected energy. The variances of the distributions of the energy values for the nonQRS-complex and QRS-com-

plex classes are of the same order. This indicates that a classification based only on the minimal distance of the cluster centra is sufficient.

A brief comparison with other algorithms has been made. The QRS-detection scheme proposed by Vary (*5*) was implemented and the results obtained from the same registrations are compared to our results. After optimization of the threshold seven FN and two FP are still found with Vary's method. For the precision of the positioning of the *R* top as detected by the algorithm, a maximal shift of 23 points was found. For the method of Goovaerts (*6*), the a priori knowledge of at least seven different templates is needed to detect all the QRS-complex shapes. Thakor's (*7*) optimal QRS detector has a familiar frequency characteristic as the combination of the characteristics of the first two blocks of the QRS-detector scheme, namely, between 10–30 Hz.

IV. Conclusion and Discussion

A robust QRS-detection algorithm is introduced. The results obtained so far are promising; only one FP and one FN is found out of 1171 QRS complexes observed. In addition, it is shown that each block of the detector contributes to the improvement of the performance. The adaptive nature of the algorithm, namely, adaptation of the cluster centra after each classification, is an important feature. It permits elimination of almost all the remaining FP.

The performance of the algorithm is not patient dependent. The involved parameters are fixed. The number of integrated samples is chosen to be 15, permitting a simple implementation on a microprocessor which is under development. This choice is not critical at all because the latest block (minimax Searcher) allows us to trim to the true *R*-top position.

Since the number of different QRS morphologies was restricted in this study, a further evaluation would be necessary. Both on-line experiments in the hospital and off-line tests on an arrhythmia data base will soon be carried out.

Acknowledgments

The authors acknowledge Mr. and Mrs. Depeursigne for providing the data and the assistance in the interpretation of the arrhythmias, Professor C. Perret of the Centre Hospitalier Univeristaire Vaudois for his collaboration, and C. Swenne of the Institute of Medical Physics (Netherlands) for valuable discussions.

References

1. Cox, J. R., Nolle, F. M., and Arthur, R. M. Digital analysis of electroencephalogram, the blood pressure wave, and the electrocardiogram. *Proc. IEEE* **60,** 1137 (1972).
2. Bonner, R. E., and Schwetman, H. D. Computer diagnosis of electrocardiograms II, a computer program for EKG measurements. *Comput. Biomed. Res.* **1,** 366 (1968).
3. Murthy, J. S. N., and Rangaray, M. R. New concepts for PVC detection. *IEEE Trans. Biomed. Eng.* **BME-26,** 409 (1979).

4. OKADA, M. A digital filter for the QRS complex detection. *IEEE Trans. Biomed. Eng.* **BME-26,** 700 (1979).
5. VARY, P. Digitale EKG-triggerung ohne multiplikationen, *Elektronik* 1980, heft 10, pp. 61–66 (1980).
6. GOOVAERTS, H. G., ROS, H. H., VAN DEN AKKER, T. J., AND SCHNEIDER, H. A digital QRS detector based on the principle of contour limiting. *IEEE Trans. Biomed. Eng.* **BME-23,** 154 (1976).
7. THAKOR, N. V., WEBSTER, J. G., AND TOMPKINS, W. J. Optimal QRS filter. IEEE Frontiers of Engineering. In *Health Care*, pp. 921–926 (1980).
8. YANOWITZ, F., KINIAS, P., RAWLING, D., AND FOZZARD, H. A. Accuracy of a continuous real-time ECG dysrhythmia monitoring system. *Circulation* **50,** 65 (1974).
9. BELFORTE, G., DE MORI, R., AND FERRARIS, F. A contribution to the automated processing of electrocardiograms using statistical methods. *In* "Pattern Recognition and signal processing." NATO Advanced Study Institute, pp. 459–483, July 1978.
10. KUNT, M., REY, H., AND LIGTENBERG, A. Preprocessing of electrocardiograms by digital techniques. *Signal Processing* **4,** 215 (1982).